Journal of Photochemistry & Photobiology, A: Chemistry 439 (2023) 114627

Contents lists available at ScienceDirect

Journal of Photochemistry & Photobiology, A: Chemistry

journal homepage: www.elsevier.com/locate/jphotochem

Synergy of UV light and heat in peptide degradation

Nikolaos Vagkidis [a], Lijuan Li [b], Jennifer M. Marsh [b], Victor Chechik [a,*]

[a] Department of Chemistry, University of York, Heslington, York YO10 5DD, UK
[b] The Procter & Gamble Company, Mason Business Center, 8700 Mason-Montgomery Road, Mason 45040, USA

ARTICLE INFO

Keywords:
Protein oxidation
Hair damage
Hydroxyl radical
Hydroperoxides
UV light
Thermal treatment

ABSTRACT

Degradation of peptides and proteins by UV light involves formation of hydroperoxide intermediates. We hypothesised that accumulation of these hydroperoxides would enhance subsequent further damage upon heating, resulting in UV and heat acting synergistically. The enhanced peptide/protein degradation is particularly relevant for dead biological tissues such as human hair, which are often subjected to alternating UV (i.e., sunlight exposure) and heat (e.g., flat ironing) treatments. The light-heat synergism hypothesis was tested using short protected peptides as protein mimics. By quantifying oxidative peptide degradation, we confirmed synergistic action of UV light and subsequent heat treatment. A combination of analytical techniques including mass spectrometry and isotope exchange experiments was used to detect and quantify hydroperoxide intermediates formed upon UV exposure. Their role in peptide degradation was further confirmed by treatment with $NaBH_4$ which destroyed hydroperoxides and increased thermal stability. Expanding these model results to a real system, we have demonstrated that thermal degradation of human hair is enhanced by the preceding treatment with solar-simulated light.

1. Background and hypothesis

Formation and accumulation of hydroperoxides (ROOH) in photochemical and thermal autoxidation processes (e.g., in environmental degradation) is well documented. [1] In organic materials such as polymers or paints, decomposition of the accumulated hydroperoxides during photothermal weathering leads to additional damage and an autocatalytic behaviour. [2–4] Autoxidation processes also take place in biological systems, and oxidative damage has been reported for different components of biological systems (such as proteins, lipids, DNA and others). [5–6] However, in living organisms the harmful effects are attenuated, at least to an extent, by defensive mechanisms. [5] Systems lacking defensive mechanisms (i.e., dead tissue such as hair and wool, foodstuffs, wood, plant seeds) are susceptible to accumulation of hydroperoxides. In this work, we aim to probe the role of these hydroperoxides in peptide/protein degradation, with particular emphasis on their relevance to hair damage.

Photothermal oxidation of dead biological systems may involve alternating thermal and photochemical exposure. For instance, human hair is often subjected to sunlight exposure followed by flat ironing. In these cases, hydroperoxides accumulated during the first insult (e.g., photochemical exposure) could lead to enhanced degradation during the second insult (e.g., thermal treatment), resulting in the synergistic action of light and heat (Scheme 1). Protein oxidation usually starts with the formation of a short-lived carbon- or sulfur-centred radical intermediate, [7] with the former being the main propagating species of protein oxidation. Most carbon-centred radicals react with O_2 (abundantly present in biological systems) with a diffusion-controlled rate ($k_{O2} = 10^9$-10^{10} M^{-1} s^{-1}) to yield peroxyl radicals (PrOO$^\bullet$). [7] In biological systems, where availability of nearby C—H bonds is high, majority of PrOO$^\bullet$ participate in hydrogen atom abstraction (HAA) to yield hydroperoxides PrOOH (typical $k_{HAA} = 10^3$ M^{-1} s^{-1}). [8] Some hydroperoxides decompose resulting in an autocatalytic behaviour but a significant amount accumulates in the system. Elevated temperatures (second insult) induce homolytic decay of hydroperoxides yielding PrO$^\bullet$ and HO$^\bullet$. These radicals are capable of further reacting with the starting (or a different) protein, thus synergistically enhancing the autoxidation.

There is some anecdotal evidence to support this synergism hypothesis, e.g., research at Procter & Gamble found higher level of hair damage in customers who use both chemical (e.g., bleaching/colouring) and thermal (e.g., flat iron) treatments than what would be expected from a simple combination of the two. However, quantitative data on the synergistic action of light and heat on protein/peptide degradation are lacking. Obtaining such data is the main objective of this work.

* Corresponding author.
E-mail address: victor.chechik@york.ac.uk (V. Chechik).

https://doi.org/10.1016/j.jphotochem.2023.114627
Received 20 December 2022; Received in revised form 6 February 2023; Accepted 8 February 2023
Available online 11 February 2023

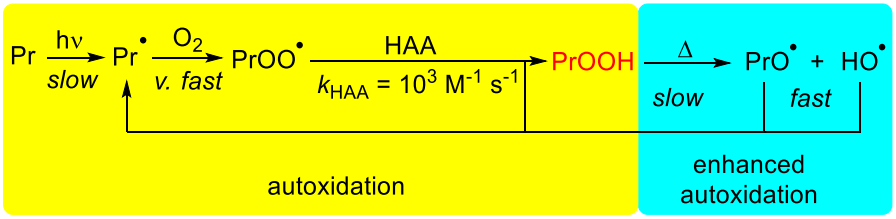

Scheme 1. Photooxidation of proteins (Pr) or lipids leads to accumulation of relatively stable hydroperoxides PrOOH. Elevated temperatures decompose the accumulated hydroperoxides yielding reactive short-lived alkoxyl and hydroxyl radicals that enhance autoxidation.

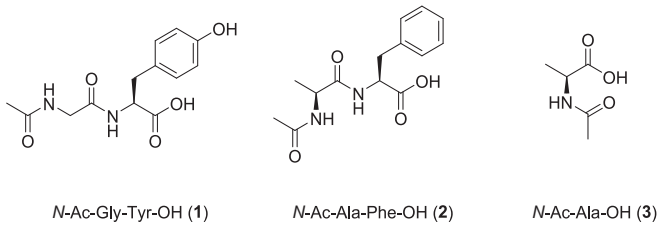

Fig. 1. Chemical structures of the three model substrates.

We chose three *N*-acetylated dipeptides/amino acids as model substrates (Fig. 1). The constituent amino acids (Tyr, Gly, Ala, Phe) form moderate amount of hydroperoxides on reaction with HO• radicals. [10] These amino acids are all found in hair keratin. [11] Tyr is one of the main chromophores responsible for photodamage of hair. Ala and Gly were chosen to probe different types of HO• reactivity: aromatic amino acids (e.g., Tyr, Phe) predominantly react by direct addition of the HO• to the ring, whereas Ala and Gly react *via* hydrogen atom abstraction. [12–15] We utilised a combination of analytical techniques to assess the parent peptide decomposition and detect and quantify hydroperoxides accumulated during photochemically-triggered oxidation of the model substrates by the HO• radical.

2. Materials and methods

2.1. Materials

Gly-Tyr-OH, Ala-Phe-OH and *N*-Ac-Ala-OH were obtained from Fluorochem. *N*-Ac-Gly-Tyr-OH and *N*-Ac-Ala-Phe-OH were synthesised according to literature protocols. [16] Xylenol orange was obtained from Merck. Ammonium Fe(II) sulfate was supplied by Merck. Catalase from bovine liver (aqueous solution; > 30 000 units per mg of protein) was supplied by Sigma Aldrich. All experiments and aqueous solutions were prepared using Milli-Q Water, or deuterium oxide (D_2O) that was supplied by Merck. Hydrogen peroxide was obtained from Fisher Scientific and was standardised using $\varepsilon_{240\ nm}$ 39.4 M^{-1} cm^{-1}. [17] Sulfuric acid and nitric acid were supplied by Fisher Scientific. All other solvents used were of analytical grade. Glassware was cleaned in concentrated nitric acid and thoroughly rinsed with Milli-Q water. This procedure was found to be essential for the removal of traces of iron. [18] Formic acid (for HPLC) and HPLC solvents were purchased from Fisher Scientific.

2.2. HO•-mediated generation and quantification of hydroperoxides

Hydroperoxides were generated by irradiation of aqueous solutions of substrates (1 mM) in the presence of aqueous H_2O_2 (100 mM) (50 mL final reaction volume) under UV light using a Philips HPK 125 W high

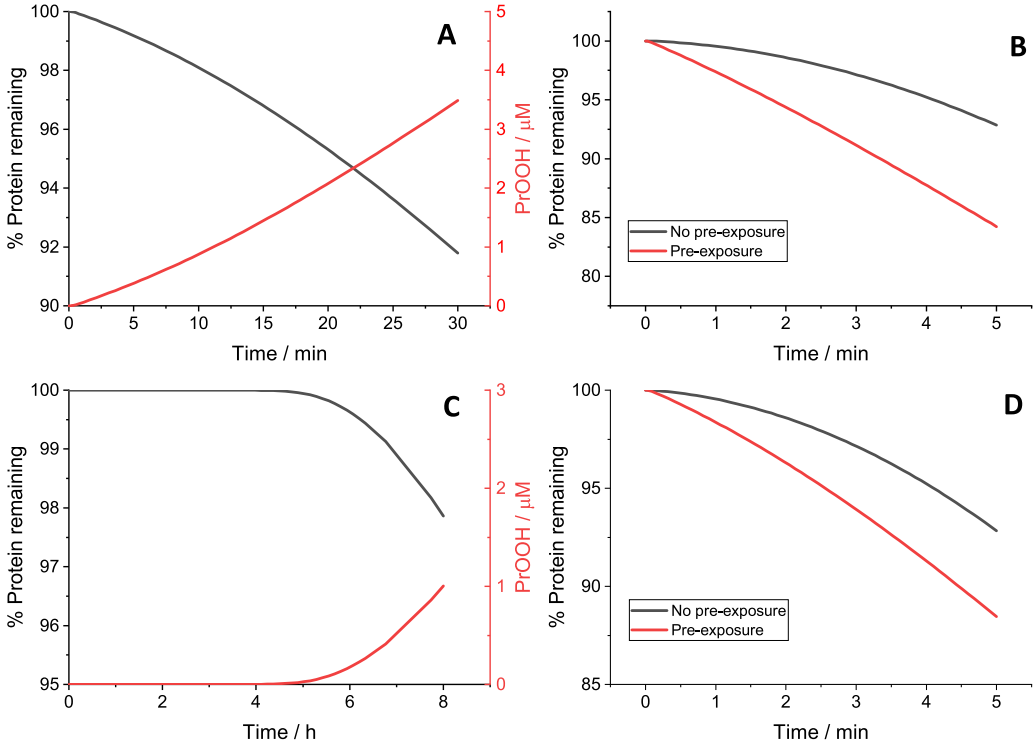

Fig. 2. Kinetic model output. A) Photooxidation of a protein and accumulation of hydroperoxides. Protein concentration was set at 1 mM, and the initiation rate was adjusted to achieve a 10 % decomposition of the starting protein after 30 min of photooxidation. B) Thermal autoxidation of a protein without (black) and following (red) photooxidation (the latter had 3.5 μM hydroperoxides at the start of the reaction). C) A slower photooxidation where 8 h of exposure led to 2 % protein decomposition. D) Evaluation of the synergistic action for the slower photooxidation (1 μM hydroperoxides at the start of the reaction).

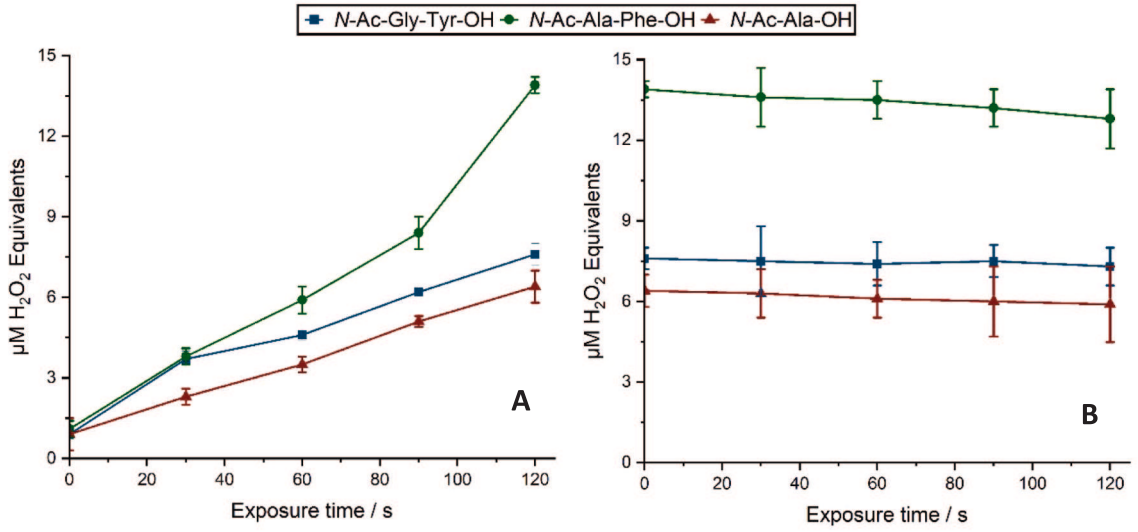

Fig. 3. A) Total hydroperoxide content in UV-treated 1 mM aq. solutions of **1**–**3** in the presence of aq. H_2O_2 (100 mM). Results are the mean ± SE of triplicate experiments (6 experiments for *N*-Ac-Ala-OH), analysed the same day with the FOX-assay. B) Loss of the hydroperoxide content observed upon exposure to UV light over 2 min. Aliquots were taken at the indicated timestamps, frozen and analysed the same day with the FOX-assay. Results are the mean ± SE of triplicate experiments, analysed the same day with the FOX-assay.

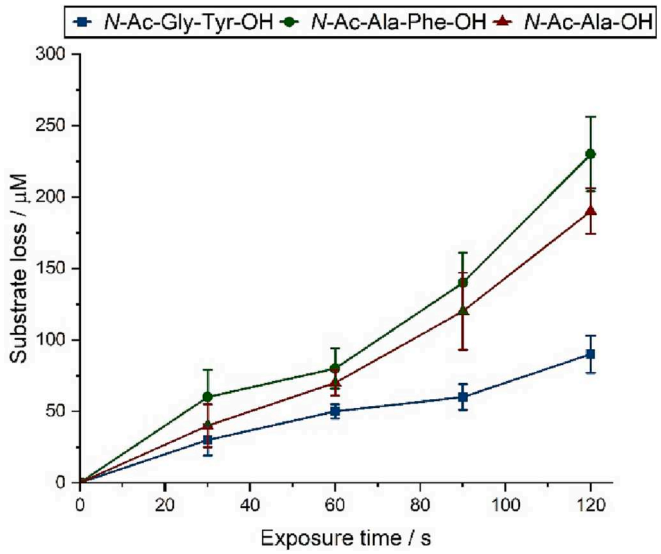

Fig. 4. Decomposition of substrates **1**–**3** in 1 mM aq. solutions upon exposure to UV light for 2 min. Aliquots were taken at the indicated timestamps and were analysed by LC-MS. The extent of decomposition was calculated by integration of the LC-MS peak of the starting peptide (the TIC of the EIC for *N*-Ac-Ala-OH). Reactions were carried out in triplicate (6 times for *N*-Ac-Ala-OH) and the results are the mean ± SE.

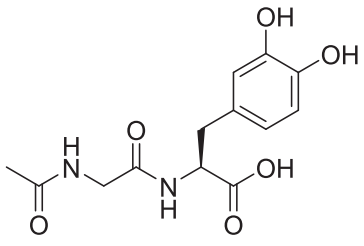

L-DOPA, exact mass 296.1008

Fig. 5. A likely structure of detected oxidation product **1**.

pressure Hg lamp with a H_2O filter (5 cm) which provides broad-band UV light. [19–20] The light output from this HP lamp provides maximum energy at 365 nm with substantial radiation also at 435, 404, 313 and 253 nm. [21] The reactions were carried out in a quartz Schlenk tube (open to air), and the flask was placed 1 cm in front of the UV lamp. The irradiance at the sample location was 32 mW/cm^2. For *N*-Ac-Gly-Tyr-OH (**1**) and *N*-Ac-Ala-OH (**3**), reactions were also run in D_2O. Aliquots (1 mL) were taken before the UV exposure and then at the indicated timestamps. Aliquots were treated with catalase (aqueous solution, 10 μL; activity 3150 U mL^{-1}) immediately after cessation of irradiation to decompose residual H_2O_2. After catalase treatment (15 min) the samples were diluted (5 mL final volume), frozen in liquid N_2 and stored in the freezer. Aliquots containing the hydroperoxides were thawed on the day of analysis. Hydroperoxides were quantified following a modified version of the FOX assay. [22] A fresh solution (assay solution) containing 4–5 mM ammonium Fe(II) sulfate and 4 mM Xylenol orange in 0.5 M H_2SO_4 was prepared every day and passed through a 0.45 μm syringe filter to remove any undissolved matter. Ammonium Fe(II) sulfate was dissolved directly in H_2SO_4 as aerobic Fe (II) oxidation is significantly slower under acidic pH. The assay solution was added to the desired peroxide sample (0.25 mL of assay solution for 5 mL of peroxide solution). The samples were gently mixed and incubated in the dark for 30 min. After that time the absorbance at 560 nm was recorded. The data were analysed using the calibration standard curve and peroxides levels are reported as H_2O_2 equivalents. The calibration curve was constructed using H_2O_2 standard solutions according to a well-established literature protocol, and can be found in the supplementary information [6].

2.3. LC-MS analysis

Separation of the parent peptides and oxidation products was performed by LC-MS using an Agilent 1200 liquid chromatography machine equipped with a reverse phase 2.7 μm Waters Correct T3 (150 × 3 mm) column and coupled to a SolariX XR FTMS 9.4 T mass spectrometer. Samples were separated at 25 °C with a flow rate of 0.2 mL min^{-1} by gradient elution. Elution solvents were: A) 0.1 % formic acid in H_2O and B) 0.1 % formic acid in MeCN. The gradient consisted of 100 % A for 5 min, 0–10 % B over 10 min, 10–30 % B over 10 min, 30 % B for 5 min, 30–5 % B over 1 min, 5 % B for 2 min, 5–0 % B over 2 min, 100 % A for 5 min.

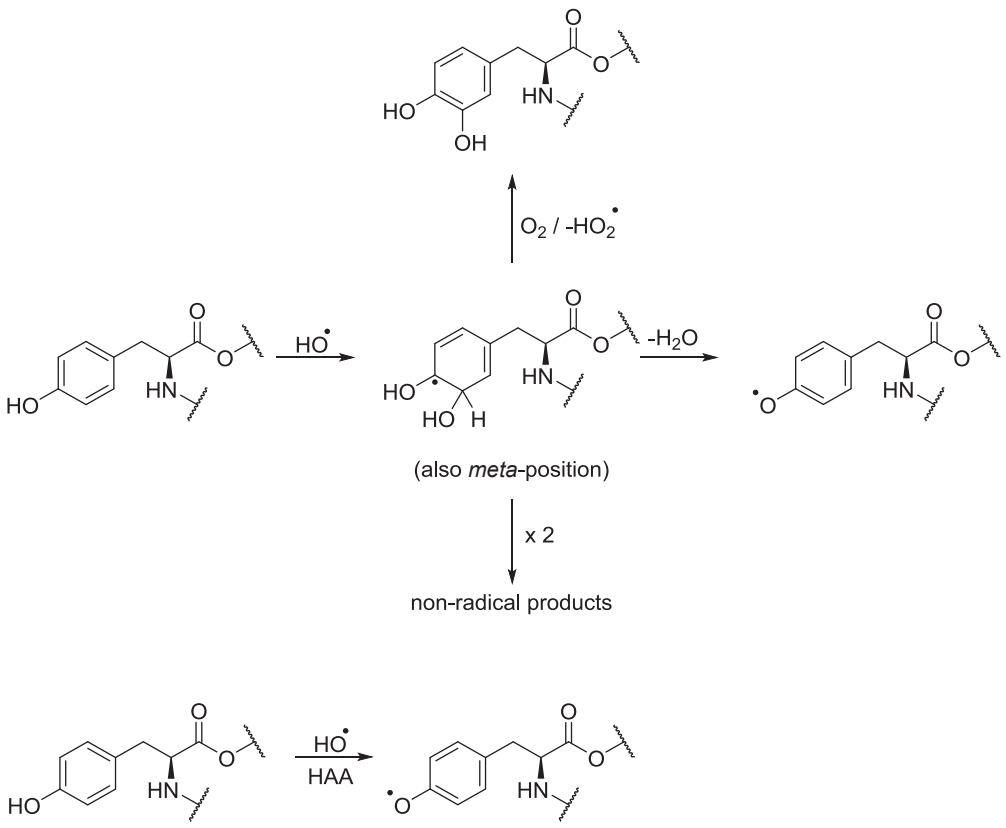

Scheme 2. Reaction between HO• and Tyr.

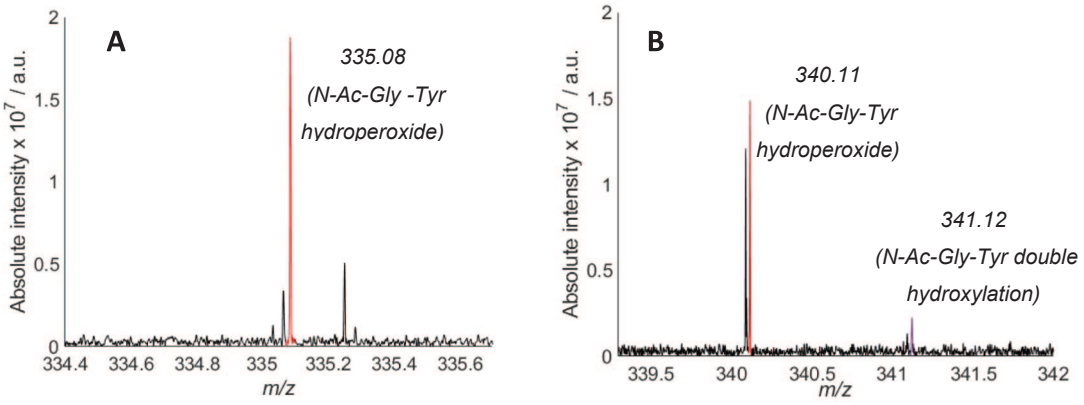

Fig. 6. Representative MS spectrum of the HO•-induced oxidation of *N*-Ac-Gly-Tyr-OH. A) Highlighted in red is the $[M + Na]^+$ peak of a potential hydroperoxide or a dihydroxylated product. B) Reactions were run in D_2O (more details under the methods section 2.6). Highlighted in red is the $[M + Na]^+$ peak corresponding to a hydroperoxide (i.e. 5 D shift in the *m/z*) and highlighted in purple is the $[M + Na]^+$ peak corresponding to a dihydroxylated species (i.e. 6 D shift in the *m/z*).

Liquid chromatography – mass spectrometry (LC-MS) calibration curves were constructed by preparing the most concentrated sample of the substrates (0.1 mM for *N*-Ac-Gly-Tyr-OH (**1**) and *N*-Ac-Ala-Phe-OH (**2**), and 1 mM for *N*-Ac-Ala-OH (**3**)), and then preparing serial dilutions (0.02 – 0.08 mM for *N*-Ac-Gly-Tyr-OH (**1**) and *N*-Ac-Ala-Phe-OH (**2**), and 0.2 – 0.8 mM for *N*-Ac-Ala-OH (**3**)). The method afforded excellent calibration curves ($R^2 > 0.997$ in all cases). For *N*-Ac-Gly-Tyr-OH (**1**) and *N*-Ac-Ala-Phe-OH (**2**), the UV detector was used and the calibration curves were constructed by integrating the peak of the peptides. For *N*-Ac-Ala-OH (**3**), the total ion count (TIC) of the $[M + H]^+$ extracted ion chromatogram (EIC) was used. All three calibration curves can be found in the supplementary information. Daily and weekly variations of the calibration curves were assessed by repeating LC-MS injections with fresh solutions for all diluted samples. For *N*-Ac-Ala-OH (**3**), reactions were carried out 6 times (as opposed to triplicate for *N*-Ac-Gly-Tyr-OH (**1**) and *N*-Ac-Ala-Phe-OH (**2**)) to account for the higher errors in the weekly variations of the calibration curve.

For direct injection MS experiments, the MS instrument was calibrated daily using a dilute solution of sodium trifluoroacetate (NaTFA) in a 1:1 $MeCN/H_2O$ mixture in a positive ion mode. The spectrometer was then flushed with a 1:1 $MeCN/H_2O$ mixture (10 μL min^{-1} for 5 min, 2 μL min^{-1} for 2 min). An average background spectrum was recorded daily. Diluted samples (×100) or undiluted for *N*-Ac-Gly-Tyr-OH (**1**) and *N*-Ac-Ala-OH (**3**) were injected in the spectrometer (2 μL min^{-1}) until stable signal was detected (typically within 10 min). A mass spectrum was then recorded, and the spectrometer was reflushed with the 1:1

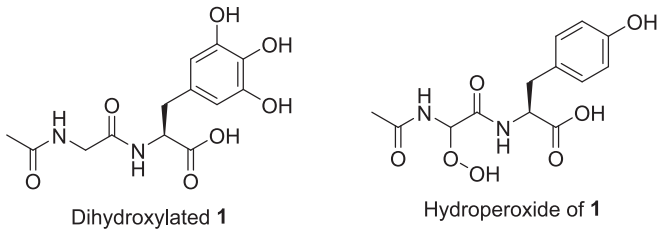

Fig. 7. Possible chemical structures of hydroperoxides or dihydroxylated oxidation products of *N*-Ac-Ala-Phe-OH (**1**). Both products share an identical mono-isotopic mass.

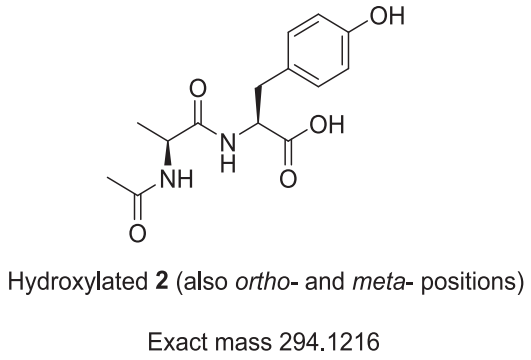

Fig. 8. Proposed structure of the detected oxidation product of *N*-Ac-Ala-Phe-OH.

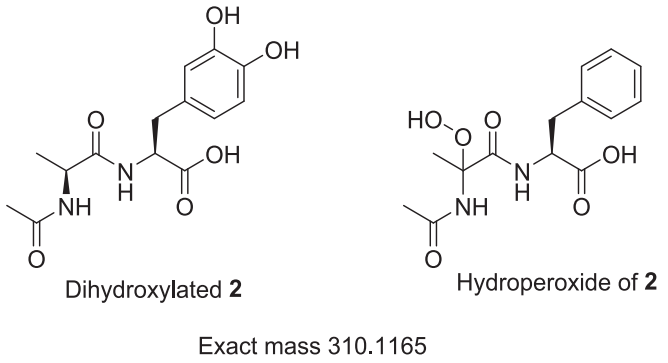

Fig. 9. Potential chemical structures of hydroperoxides or dihydroxylated oxidation products of *N*-Ac-Ala-Phe-OH. Both products share an identical mono-isotopic mass.

MeCN/H_2O mixture and the procedure was repeated.

2.4. Thermal treatment of irradiated solutions

At the end of the UV irradiation, the remainder of the solution (45 mL) was treated with catalase (10 μL; similarly to the hydroperoxide quantification section 2.2). After 15 min, the H_2O_2-free solutions were incubated at 82 °C for 30 min. After this time, one aliquot (1 mL diluted to 5 mL final volume) was analysed by the FOX-assay to determine the total hydroperoxide content, and one aliquot (0.01 mL diluted to 1 mL for *N*-Ac-Gly-Tyr-OH (**1**) and *N*-Ac-Ala-Phe-OH (**2**), and 0.1 mL diluted to 1 mL for *N*-Ac-Ala-OH (**3**)) was analysed by LC-MS to determine the parent substrate concentration.

2.5. MS/MS studies

For MS/MS, He was used as the collision gas for collision-induced dissociation (CID) experiments to generate fragments, with a normalized collision energy of 10 or 15 %. Detected ions on MS analysis with masses $[M + 32 + H]^+$ (potential hydroperoxides) and $[M + 16 + H]^+$ (potential alcohols) were subjected to MS/MS and the resulting fragments ions were analysed.

2.6. Deuterium exchange studies

Irradiated solutions (1 mL) were diluted (×100) in D_2O. Solutions were left in the dark for 1 h before analysis by direct injection MS and LC-MS as indicated in the materials and methods (section 2.3). A 1 h incubation in D_2O was determined to be sufficient to exchange all labile H of the starting substrates (reagent in excess) with D atoms. Alternatively, the reactions were performed in D_2O (instead of Milli-Q H_2O) to enable more concentrated solutions to be injected (while ensuring complete exchange of all labile H).

2.7. Sodium borohydride treatment

Photo-generated hydroperoxides were reduced by treatment with solid $NaBH_4$ (1 mg per mL of solution). Solutions were left to incubate in the dark for 1 h, before lowering the pH of the solutions to 2 using aq. 1 M HCl, to neutralise the remaining $NaBH_4$. The pH of the solutions was then restored to 6 using aq. 1 M NaOH. The total hydroperoxide content was determined by FOX-assay and showed complete disappearance of hydroperoxides.

2.8. Hair source and treatment

Light blonde human hair for the testing was purchased from International Hair Importers & Products, Glendale, NY. Tresses of hair (1.5 g, 15 cm) were either subjected to sunlight or heat or a combination of both and then sampled for biomarker analysis (3 tresses per test, 3 samples of hair taken per tress). Sun exposure was simulated by irradiation with an Atlas Ci3000+ weather-o-meter (Atlas, Chicago, Illinois, US). An internal and outer quartz filter was used to simulate broad-spectrum, outdoor daylight with a specific irradiance of 1.48 W/m^2 at 420 nm. During the irradiation process, temperature, and relative humidity (RH) were kept constant at 35 °C and 80 % RH, respectively. Heat application was *via* a flat-iron at 200 °C, 5 cycles of 3 passes.

2.9. Biomarker measurement

Samples (0.5 g) of hair from treated tresses were cut and placed into 50 mL tubes with 5 mL of water added. Tubes with hair and water were mixed on a multi-tube vortex shaker for 60 min at 2500 rpm. Water portion was then transferred from the tubes by pipette into glass scintillation vials. A 10 mg/mL solution of MALDI matrix (alpha-cyano-4-hydroxy cinnamic acid) was mixed with the hair extract samples in a 1:1 vol ratio. A 1 μL of this solution was used to spot onto the MALDI plate and MALDI MS spectra was acquired (1000 shots). Intensity of the UV damage marker peptide at *m/z* 1278 was measured.

3. Results and discussion

3.1. A simplified kinetic model of protein degradation

In order to test the scope and feasibility of the proposed synergism, we constructed a simplified kinetic model of protein autoxidation based on Scheme 1 with some additional reactions (full list of reactions incorporated in the model can be found in the supplementary data). The kinetic model was designed and run using the Kintecus software. [9] Due to lack of reliable kinetic data on protein hydroperoxide decomposition

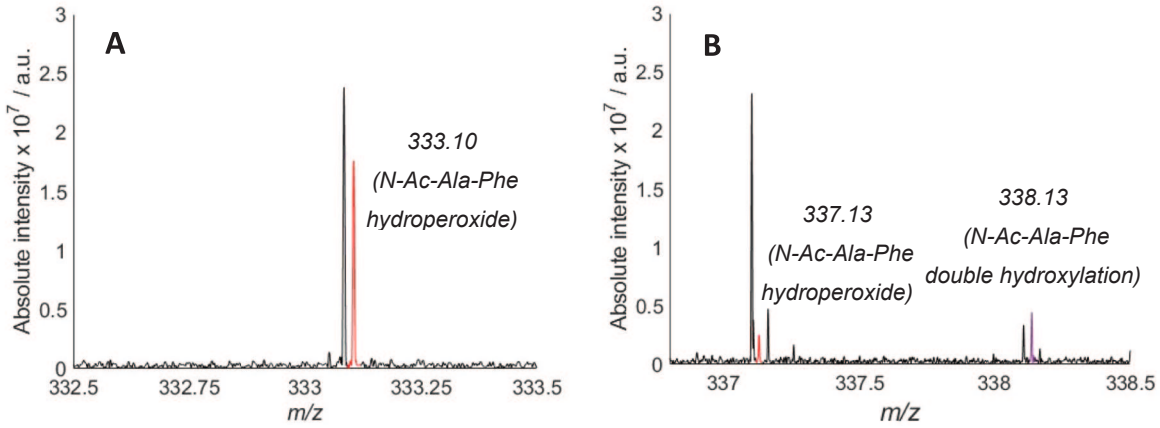

Fig. 10. Representative MS spectrum of the HO•-induced oxidation of *N*-Ac-Ala-Phe-OH. A) Highlighted in red is the $[M + Na]^+$ peak of a potential hydroperoxide or a dihydroxylated product. B) Aliquots were diluted × 100 in D_2O (more details under the methods section 2.6). Highlighted in red is the $[M + Na]^+$ peak corresponding to a hydroperoxide and highlighted in purple is the $[M + Na]^+$ peak corresponding to a dihydroxylated species.

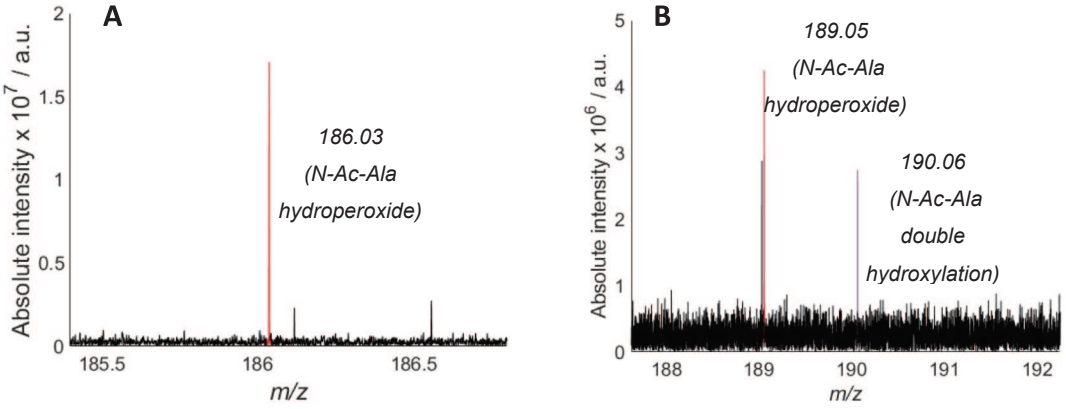

Fig. 11. MS spectra of the HO•-induced oxidation of *N*-Ac-Ala-OH. A) The peak corresponding to a hydroperoxide or a dihydroxylated product is highlighted in red. B) Reaction was carried out in D_2O (more details under the methods section 2.6). Highlighted in red is the $[M + Na]^+$ peak corresponding to a hydroperoxide and highlighted in purple is the $[M + Na]^+$ peak corresponding to a dihydroxylated species.

in the literature, we experimentally determined the rate constant for the decay of hydroperoxides formed in an aqueous solution of *N*-Ac-Gly-Gly (5 mM) upon exposure to simulated sunlight (10^{-4} s^{-1}; data in the supplementary information).

The model was used to estimate accumulation of hydroperoxides in a protein upon exposure to UV light. Initially, the rate of photoinitiation was adjusted to achieve ca. 10 % decomposition of the protein (at 1 mM concentration) over a 30 min simulation period (Fig. 2A; left Y axis). The results show a continuous growth of hydroperoxides (PrOOH) (Fig. 2A; right Y axis). The concentration of hydroperoxides would plateau and then decay at much longer exposure times. The results of this simulation are in a reasonable agreement with our experimental data on HO•-mediated decomposition of 3 model substrates (*vide infra*).

In order to test the synergistic action hypothesis, the system without and with accumulated hydroperoxides (at the end of simulation in Fig. 2A) was exposed to elevated temperature (100 °C) for 5 min (Fig. 2B). The results in Fig. 2B indeed show enhanced thermal degradation of protein which was pre-exposed to UV light. This effect (enhanced protein degradation) is strongest at the beginning of thermal treatment (within the first 2 min). This can be easily explained by the fact that at longer exposure times, the sample which was not pre-exposed to UV light would accumulate hydroperoxides to a similar level to the pre-treated sample, and the two samples would then degrade at similar rates.

The effect was also tested at a much slower photoinitiation rate (ca. 2 % protein degradation after 8 h light exposure) that would be much closer to a real-life scenario. The rates of other photochemical steps were reduced accordingly. The model predicted a considerably slower accumulation of hydroperoxides with nearly 1 μM at the end of the 8 h simulation (Fig. 2C; right Y axis). Importantly, the sample pre-exposed to UV light also showed enhanced degradation compared to the untreated control (Fig. 2D).

3.2. Formation and quantification of hydroperoxides

Hydroperoxides were generated by reacting the three substrates with HO• formed by photolysis of H_2O_2. The photolytically generated HO• participates in hydrogen atom abstraction (HAA) reactions with peptides with near diffusion controlled second order rate constants, leading to the formation of carbon-centred radicals (R•), [23] which react with oxygen (Scheme 1) eventually forming hydroperoxides among other products. In solutions where H_2O_2 is in large excess, reaction between HO• and H_2O_2 can also occur ($k_3 = 2.7 \times 10^7$ M^{-1} s^{-1}) [24] generating a less reactive hydroperoxyl radical ($HO_2^{\bullet}$) Hydroperoxyl radical is capable of reacting with organic molecules *via* HAA ($k_4 \sim 10^2$ M^{-1} s^{-1}) to produce a carbon-centred radical R• and H_2O_2. [25].

Reactions were run in a 100-fold excess of H_2O_2 in order to reduce the likelihood of direct absorption of UV light by the protected peptides

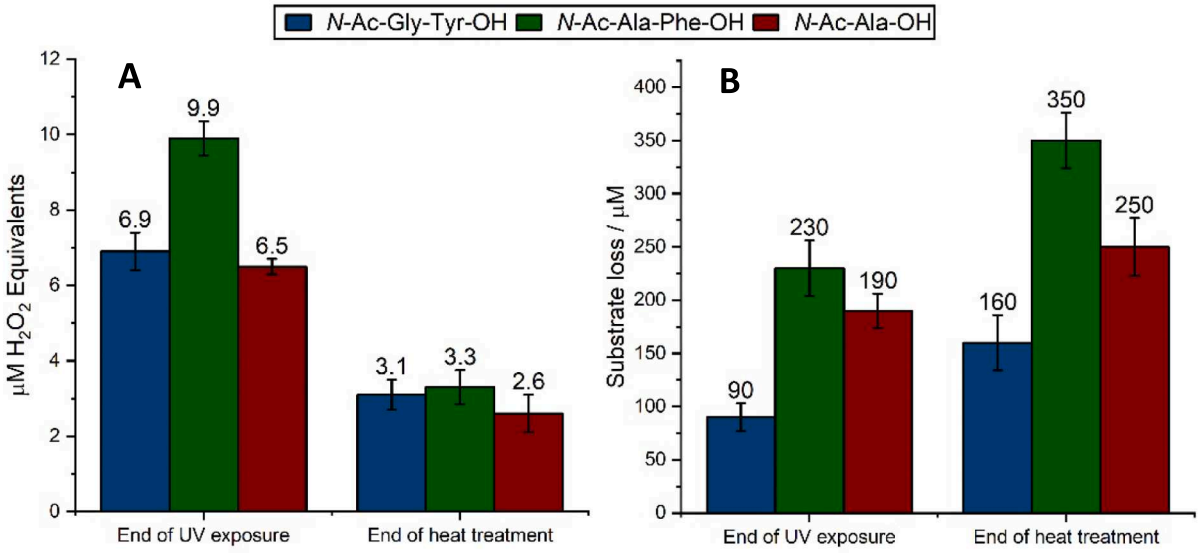

Fig. 12. A) Hydroperoxide content at the end of the UV exposure and at the end of the consequent thermal treatment at 82 °C for 30 min. Results are the mean ± SE of three (six for *N*-Ac-Ala-OH) separate experiments analysed by the FOX-assay on the same day. B) Substrate degradation at the end of the UV irradiation and the end of the thermal treatment at 82 °C for 30 min. Data are expressed as the means of percentage initial substrate concentration ± SE of 3 separate experiments (6 for *N*-Ac-Ala-OH) analysed by LC-MS.

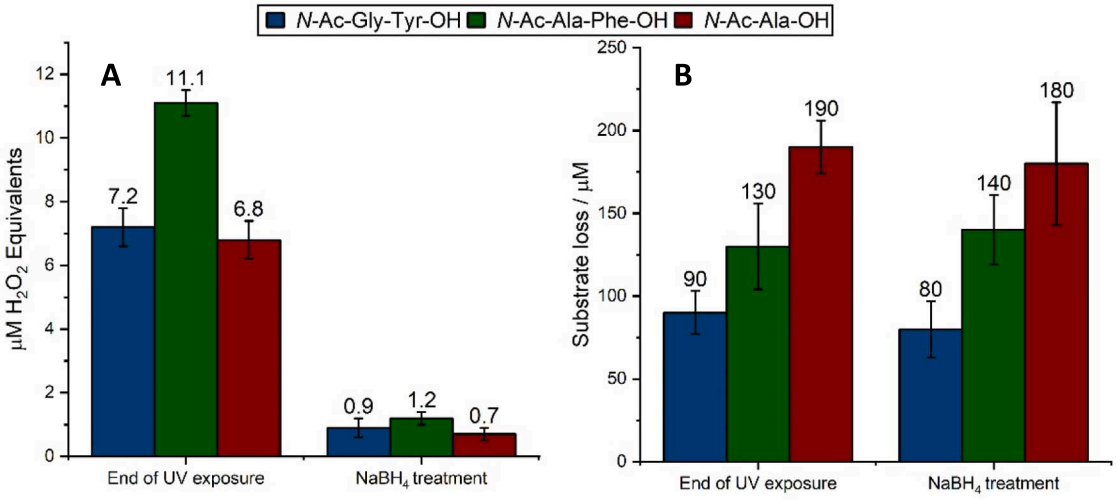

Fig. 13. A) Decomposition of HO•-generated peroxides in the three substrates under study after UV exposure. Aliquots were treated with $NaBH_4$ (1 mg per 1 mL of solution) and were incubated in the dark for 1 h. Results are the mean ± SE of three separate experiments analysed by the FOX-assay the same day. B) Degradation of the three substrates at 82 °C. Solutions were initially exposed to UV light for 2 min. After the cessation of irradiation, samples were treated with $NaBH_4$ (1 mg per 1 mL of solution) to reduce any photo-generated hydroperoxides to alcohols, and incubated at 82 °C for 30 min. Data are expressed as the means of percentage initial substrate concentration (3 experiments for **1** and **2**, 6 experiments for **3**) ± SE.

or their hydroperoxides. A control UV irradiation experiment under the same reaction conditions but in the absence of H_2O_2 confirmed no detectable peptide degradation (data not shown). The total hydroperoxide yields were determined by FOX-assay (Fig. 3A).

The yield of hydroperoxides for *N*-Ac-Ala-Phe-OH (**2**) was the highest of all substrates at *ca.* 15 μM after 2 min of irradiation. This is consistent with literature reports suggesting that Ala and Phe are more efficient at generating hydroperoxides compared to Gly and Tyr. [10] *N*-Ac-Gly-Tyr-OH (**2**) and *N*-Ac-Ala-OH (**3**) gave an intermediate yield of hydroperoxides at the end of the irradiation (*ca.* 7 μM in both cases).

Accumulated hydroperoxides can also undergo photolysis yielding alkoxyl and hydroxyl radicals. To estimate the efficiency of UV decomposition of hydroperoxides formed during irradiation in our system, solutions were treated with catalase to destroy excess H_2O_2, before irradiating them for another 2 min. Aliquots were taken every 30 s, and the total peroxide content was determined by the FOX assay. The results (Fig. 3B) suggests that hydroperoxides are reasonably stable under irradiation, with only a very small loss at the end of the 2 min exposure. This is consistent with the continuous increase of hydroperoxide content in Fig. 3A, as significant hydroperoxide degradation would have led to its plateauing.

3.3. Peptide decomposition monitored by LC-MS analysis

Degradation of substrates **1**–**3** by reaction with HO• radicals was quantified using LC-MS (Fig. 4). The quantification assumed constant ionisation efficiency in ESI-MS. While this is not normally a safe assumption, at low conversions the composition of the reaction mixtures

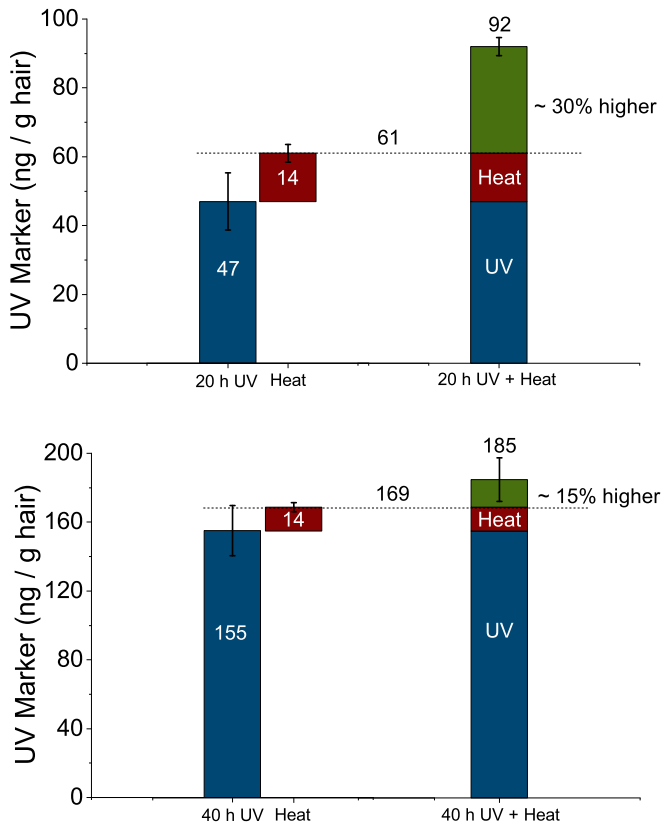

Fig. 14. Evolution of UV marker upon exposure of hair to UV light for 20 or 40 h and further heat-treatment. Results are the mean ± SE of 12 different experiments.

is almost constant, and big changes in ionisation efficiency over reaction time would not be expected.

A relatively small (but clearly noticeable) proportion of the substrates was degraded under reaction conditions. *N*-Ac-Ala-Phe-OH (**2**) and *N*-Ac-Ala-OH (**3**) degrade with a similar rate resulting in a *ca.* 20 % decomposition at the end of the irradiation. In contrast, *N*-Ac-Gly-Tyr-OH (**1**) showed considerably lower decomposition with only a 10 % loss. This can be rationalised by the fact that oxidation of **1** predominantly yields a phenoxyl radical which is unlikely to propagate peptide damage (as its reaction with O_2 to form a peroxyl radical is a minor pathway, *vide infra*).

3.4. Detection of peptide hydroperoxides

In order to get better understanding of the oxidation mechanism and confirm formation of peptide hydroperoxides, reaction mixtures were analysed by direct injection MS and LC-MS.

3.4.1. N-Ac-Gly-Tyr-OH

The major detected oxidation product of *N*-Ac-Gly-Tyr-OH (**1**) was its hydroxylated derivative (i.e., L-DOPA or another isomer, Fig. 5).

This is consistent with literature studies that have concluded that reaction between HO$^\bullet$ and Tyr involves predominantly direct addition to the aromatic ring (overall $k_{add} = 1.5 \times 10^{10}$ M^{-1} s^{-1}), and L-DOPA is the only observed oxidation product. [15] The initial addition of HO$^\bullet$ yields transient dihydroxy-cyclohexadienyl radicals (Scheme 2), which undergoes spontaneous H_2O elimination to give a more stable phenoxyl radical. [12,26–27].

HO$^\bullet$ addition to the *ortho*- and *meta*-positions of the phenol ring (50 % and 30 % of the initial HO$^\bullet$, respectively) has rate constants of $k_{ortho} = 7.0 \times 10^9$ M^{-1} s^{-1} and $k_{meta} = 5.0 \times 10^9$ M^{-1} s^{-1}. [12] HAA from the phenol accounts only for about 5 % of the initial HO$^\bullet$ with a $k_{HAA} = 5.0 \times 10^3$ M^{-1} s^{-1}. [12] The remaining 10 % of the HO$^\bullet$ is suggested to involve all other possible reaction processes, such as HO$^\bullet$ addition to the *ipso*- positions, while HAA from the –CH_2 position is negligible. [12,26].

Both *ortho*- and *meta*-cyclohexadienyl adducts can undergo rapid and reversible O_2 addition ($k_f \sim 10^8$ M^{-1} s^{-1}, $k_r \sim 10^4$ s^{-1}) with subsequent $HO_2^\bullet$ elimination ($k_{HO2} \sim 10^3$ s^{-1}) which generates L-DOPA as the main oxidation product. [28] Radical-radical reactions to afford non-radical products are fast ($2k \sim 2 \times 10^9$ M^{-1} s^{-1}). [12] Reaction of phenoxyl radicals with O_2 is slow ($k < 10^3$ M^{-1} s^{-1} for tyrosyl phenoxyl radicals) [29] and hence only a very low concentration of hydroperoxides is formed during the irradiation.

Nonetheless, HAA from the glycine moiety of *N*-Ac-Gly-Tyr-OH (**1**) by HO$^\bullet$ can lead to the generation of hydroperoxides. Indeed, the $[M + Na]^+$ peak corresponding to potential hydroperoxides was detected in the direct injection MS spectra (Fig. 6A; highlighted in red), while non-irradiated samples showed no evidence of this product (data not shown).

It is important to highlight that the mono-isotopic mass of hydroperoxides of **1** is identical to that of a dihydroxylated oxidation product (Fig. 7). In order to distinguish between the hydroperoxides and dihydroxylated products, deuterium exchange experiments were carried out (more information under the methods section 2.6), as these compounds possess a different number of exchangeable protons (5 and 6 for hydroperoxides and dihydroxylated products of *N*-Ac-Gly-Tyr-OH, respectively). No peaks associated with 0–4 D shifts were detected in the MS spectra. However, the peaks with *m/z* corresponding to 5 and 6 D shifts were evident (Fig. 6B). These data strongly support formation of both hydroperoxide and dihydroxylated products for *N*-Ac-Gly-Tyr-OH (**1**).

3.4.2. N-Ac-Ala-Phe-OH

N-Ac-Ala-Phe-OH (**2**) was also expected to predominantly undergo addition of HO$^\bullet$ radical to the aromatic ring. As such, the primary oxidation product should be a hydroxylated derivative (Fig. 8). The corresponding peak was indeed clearly seen in the MS of the oxidation mixture.

The phenol in Fig. 8 has the same mono-isotopic mass as a product of Ala hydroxylation. MS/MS studies showed that both products are formed (supplementary information). The hydroxylated Ala product is likely produced *via* a hydroperoxide decomposition, and its observation thus indirectly supports intermediate formation of hydroperoxides. We note that aliphatic residues can also be hydroxylated *via* dismutation of two ROO$^\bullet$ radicals (Russell mechanism), although the latter mechanism is only applicable to primary or secondary peroxyls. [30].

In order to probe the formation of hydroperoxides and isomeric dihydroxylation products (Fig. 9), reactions were analysed by LC- and direct injection MS.

Literature data suggest that HO$^\bullet$ adds primarily to Phe in the *ortho*-position (50 % of the initial HO$^\bullet$ concentration) with a $k_{ortho} = 3.5 \times 10^9$ M^{-1} s^{-1}, followed by addition to the *para*- and the *meta*-position (30 % and 14 % of the initial HO$^\bullet$ respectively) with $k_{para} = 2.2 \times 10^9$ M^{-1} s^{-1} and $k_{meta} = 1.0 \times 10^9$ M^{-1} s^{-1}. [26] The remaining HO$^\bullet$ (6 %) reacts with the –CH_2 group *via* a HAA reaction with a $k_{abs} = 9 \times 10^8$ M^{-1} s^{-1}. [26] This generates a carbon centred radical that would react readily with O_2. In addition, a C-centred radical can be formed by HAA from the CH group of Ala. Hence *N*-Ac-Ala-Phe-OH (**2**) was expected to give a higher yield of hydroperoxides than *N*-Ac-Gly-Tyr-OH (**1**).

The $[M + Na]^+$ peak corresponding to a hydroperoxide or a dehydroxylated product was indeed detected in the direct injection MS spectra (Fig. 10A; highlighted in red), while non-irradiated samples showed no evidence of this product (data not shown). Deuterium exchange experiments showed no *m/z* for 0–3 D shifts, but the peaks corresponding to 4 (hydroperoxide) and 5 D (dehydroxylated product) shifts were evident (Fig. 10B), strongly suggesting formation of both species.

3.4.3. N-Ac-Ala-OH

As *N*-Ac-Ala-OH (**3**) does not have an aromatic ring, its predominant reaction with HO$^{\bullet}$ is HAA which ultimately yields a hydroperoxide. [30] The HAA is expected to predominantly occur at the α-carbon yielding a relatively stable tertiary radical that is stabilised by the neighbouring amide and carbonyl functionalities. [31–34].

Hydroperoxide decomposition leads to the formation of an alcohol, and thus detection of hydroxylated *N*-Ac-Ala-OH (**3**) indirectly supports hydroperoxide formation (supplementary information). An alternative pathway to the alcohol *via* ROO$^{\bullet}$ dismutation (Russell mechanism) is unlikely as this mechanism is only applicable to primary or secondary peroxyl radicals.

Direct injection MS showed an $[M + Na]^+$ peak of a hydroperoxide/dihydroxylated derivative (Fig. 11A). Deuterium exchange studies confirmed formation of both products, hydroperoxide with 3 D shift, and a diol with 4 D shift (Fig. 6B). Formation of hydroperoxides was thus confirmed for all three model substrates.

3.5. Investigation of the synergism hypothesis

To evaluate the proposed synergistic effect of light and heat on the peptide decomposition, light-exposed peptide solutions (after decomposition of H_2O_2 with excess catalase) were incubated at 82 °C for 30 min. At the end of thermal treatment, they were analysed by the FOX-assay. This allowed us to determine that for all three substrates, total hydroperoxide content is substantially reduced at elevated temperatures (Fig. 12A).

The heated samples were also analysed by LC-MS to assess the decay of the parent substrates. Thermal treatment resulted in further damage to the light-exposed substrates (Fig. 12B). We note that when solutions of the substrates were incubated at 82 °C without pre-exposure to UV light and in the absence of H_2O_2, no appreciable decomposition was detected (supplementary information). These data strongly support the proposed synergism hypothesis: hydroperoxides accumulated during irradiation lead to enhanced degradation during consequent thermal treatment. Although other unstable oxidation products could also contribute to the increased damage upon heat treatment, high reactivity of alkoxyl radicals formed from hydroperoxides is likely to make them the main propagating species.

3.6. Sodium borohydride reduction of peroxides

In order to further confirm the role of accumulated hydroperoxides in peptide oxidation, we sought to selectively destroy the hydroperoxides *via* a non-radical pathway. This can be done by a number of reducing agents. [10] In particular, $NaBH_4$ decomposes hydroperoxides to the corresponding alcohols under mild conditions (e.g., 1 h incubation at room temperature). Many studies utilised $NaBH_4$ for quantification of protein/peptide hydroperoxides by reduction to alcohols. [35–37].

In order to test the efficiency of the method, aqueous solutions of the substrates were exposed to UV light as described earlier. At the end of the irradiation, the solutions were treated with catalase to remove any leftover H_2O_2. An aliquot was analysed by both the FOX-assay and LC-MS, in order to determine the total hydroperoxide content and the starting substrate concentration. The remainder of the solutions was treated with $NaBH_4$ (1 mg per 1 mL of solution) for 1 h to reduce any UV-generated hydroperoxides to alcohols. These mixtures were also analysed by the FOX-assay (Fig. 13A). The results confirmed that $NaBH_4$ treatment resulted in a significant reduction of the total hydroperoxide content.

After the $NaBH_4$ treatment, all solutions were subjected to heat-treatment as described earlier (82 °C; 30 min) (Fig. 13B). Fig. 13B demonstrates that all three substrates remained intact upon thermal-treatment. This strongly supports our conclusion that the degradation of light-exposed substrates in Fig. 12B is due to the accumulation of hydroperoxides, and provides further evidence for the synergistic effect of light and heat in peptide degradation.

4. Evaluation of the synergistic action on human hair

Encouraged by these results, we sought to investigate whether this effect could be detected in human hair. We note that hair chemistry is much more complex than that of simple peptides and is additionally affected by the presence of lipids, melanin granules, morphology etc. Nonetheless we argued that accumulation of hydroperoxides upon light exposure followed by their degradation during heat treatment could be observed even in complex systems. As such, hair samples were exposed to simulated sunlight for 20 and 40 h (more details under the methods section 2.8), before applying heat-treatment. Protein degradation was assessed by monitoring a UV marker with m/z 1278.7 which originates from the calcium-binding protein S100A3. We have previously reported a linear correlation between UV exposure of hair and generation of this marker. [38] It is likely formed *via* peptide bond cleavage which involves intermediate formation of a hydroperoxide. It is assumed that some copper ions (which catalyse decomposition of hydroperoxides) can exchange with calcium at S100A3 binding site, which explains selective cleavage of this fragment. The evolution of the UV marker is thus associated with the oxidation of hair protein.

The results (Fig. 14) suggest that evolution of the UV marker upon 20 h of UV exposure followed by heat-treatment (20 h UV + Heat) is greater than the combined effect of the two insults (heat and 20 h UV). This is consistent with our work on short peptides and indicates that exposure of hair to UV light generates thermally unstable hydroperoxides that decay at elevated temperatures to yield transient radicals, which in turn accelerate protein damage.

The effect at 40 h of UV exposure is less clear and the errors are higher. This is however not surprising. Our kinetic model showed a similar trend, where at longer irradiation times the prooxidant effect of hydroperoxides is attenuated. We believe that after an initial period of hydroperoxide accumulation, a steady state concentration is reached as hydroperoxides are formed and decomposed simultaneously (Fig. 2B and 1D). Therefore, it is likely that the total peroxide content at the end of the 40 h exposure is similar to that at the end of the 20 h exposure.

5. Conclusions

The HO$^{\bullet}$/O_2-mediated oxidation of *N*-Ac-Gly-Tyr-OH (**1**), *N*-Ac-Ala-Phe-OH (**2**) and *N*-Ac-Ala-OH (**3**) resulted in accumulation of hydroperoxides. The total peroxide content was determined by the FOX-assay, while the evidence for the formation of hydroperoxides was obtained for all three substrates using LC-MS, direct injection MS and MS/MS. In all cases, D_2O exchange studies further supported this conclusion. At elevated temperatures, hydroperoxides decay and give rise to free radicals which cause further oxidative damage to the parent substrate. This is confirmed by the quantification of the parent substrate concentration by LC-MS which revealed that thermal treatment of irradiated solutions accelerates the damage.

We believe that this mechanism is relevant to oxidation of dead biological tissue including hair. Experimental data on human hair degradation were consistent with the conclusion that UV light and heat-treatment act together in synergy to accelerate damage on hair proteins.

CRediT authorship contribution statement

Nikolaos Vagkidis: Writing – original draft, Methodology, Investigation. **Lijuan Li:** Methodology. **Jennifer Marsh:** Writing – original draft, Supervision, Resources, Funding acquisition, Conceptualization. **Victor Chechik:** Writing – original draft, Supervision, Project administration, Funding acquisition, Conceptualization.

Declaration of Competing Interest

The authors declare that they have no known competing financial interests or personal relationships that could have appeared to influence the work reported in this paper.

Data availability

Raw data used in this paper is available at https://doi.org/10.15124/d9e75138-5055-4ed7-a7ae-6188136ec8eb.

Acknowledgements

The authors would like to thank The Procter & Gamble Company and University of York for support of this work.

Appendix A. Supplementary data

Supplementary data to this article can be found online at https://doi.org/10.1016/j.jphotochem.2023.114627.

References

[1] M.L. Janssens, Handbook of Environmental Degradation of Materials, 3rd edn., William Andrew Publishing, 2005.
[2] D.F. Mielewski, D.R. Bauer, J.L. Gerlock, Polym. Degrad. Stab. 33 (1991) 93–104.
[3] T. Ojeda, A. Freitas, K. Birck, E. Dalmolin, R. Jacques, F. Bento, F. Camargo, Polym. Degrad. Stab. 96 (2011) 703–707.
[4] J. Lemaire, R. Arnaud, J.L. Gardette, Pure Appl. Chem. 55 (1983) 1603–1614.
[5] B. Halliwell, J.M.C. Gutteridge, Free Radicals in Biology and Medicine, Oxford University Press, 2015.
[6] C.L. Hawkins, P.E. Morgan, M.J. Davies, Free Radic. Biol. Med. 46 (2009) 965–988.
[7] M.J. Davies, Biochem. J. 473 (2016) 805–825.
[8] P. Neta, R.E. Huie, A.B. Ross, J. Phys. Chem. Ref. Data 19 (1990) 413–513.
[9] J. C. Ianni, in *Computational Fluid and Solid Mechanics 2003*, ed. K. J. Bathe, Elsevier Science Ltd, Oxford, UK, 2003, pp. 1368–1372.
[10] S. Gebicki, J.M. Gebicki, Biochem. J. 289 (1993) 743–749.
[11] C. Popescu, H. Höcker, Chem. Soc. Rev. 36 (2007) 1282–1291.
[12] S. Solar, W. Solar, N. Getoff, J. Phys. Chem. 88 (1984) 2091–2095.
[13] C.L. Hawkins, M.J. Davies, Biochim. Biophys. Acta Bioenerg. 1504 (2001) 196–219.
[14] G. Xu, M.R. Chance, Chem. Rev. 107 (2007) 3514–3543.
[15] X.R. Liu, M.M. Zhang, B. Zhang, D.L. Rempel, M.L. Gross, Anal. Chem. 91 (2019) 9238–9245.
[16] K. Drauz, G. Knaup, U. Groeger, N-acyl Dipeptides and their Compositions, US Patent No. US5534538A, 1996.
[17] D.P. Nelson, L.A. Kiesow, Anal. Biochem. 49 (1972) 474–478.
[18] C. Gay, J.M. Gebicki, Anal. Biochem. 284 (2000) 217–220.
[19] D.P. Dickinson, S.W. Evans, M. Grellier, H. Kendall, R.N. Perutz, B. Procacci, S. Sabo-Etienne, K.A. Smart, A.C. Whitwood, Organometallics 38 (2019) 626–637.
[20] B. Procacci, S.B. Duckett, M.W. George, M.W.D. Hanson-Heine, R. Horvath, R. N. Perutz, X.Z. Sun, K.Q. Vuong, J.A. Welch, Organometallics 37 (2018) 855–868.
[21] HPK125W - Hi-Tech Lamps, Inc., https://www.hi-techlamps.com/hpk125w/, (accessed 23 February 2020).
[22] P.E. Morgan, D.I. Pattison, C.L. Hawkins, M.J. Davies, Free Radic. Biol. Med. 45 (2008) 1279–1289.
[23] G.V. Buxton, C.L. Greenstock, W.P. Helman, A.B. Ross, J. Phys. Chem. Ref. Data 17 (1988) 513–886.
[24] P. Kralik, H. Kusic, N. Koprivanac, A. Loncaric Bozic, Chem. Eng. J. 158 (2010) 154–166.
[25] B.H.J. Bielski, D.E. Cabelli, R.L. Arudi, A.B. Ross, J. Phys. Chem. Ref. Data 14 (1985) 1041–1100.
[26] N. Getoff, Amino Acids 2 (1992) 195–214.
[27] C. von Sonntag, J. Chem. Society, Perkin Trans. 2 (2001) 264–268.
[28] X. Fang, X. Pan, A. Rahmann, H.-P. Schuchmann, C. von Sonntag, Chem. – A Eur. J. 1 (1995) 423–429.
[29] E.P.L. Hunter, M.F. Desrosiers, M.G. Simic, Free Radic. Biol. Med. 6 (1989) 581–585.
[30] P.E. Morgan, D.I. Pattison, M.J. Davies, Free Radic. Biol. Med. 52 (2012) 328–339.
[31] S. Fu, L.A. Hick, M.M. Sheil, R.T. Dean, Free Radic. Biol. Med. 19 (1995) 281–292.
[32] Z.I. Watts, C.J. Easton, J. Am. Chem. Soc. 131 (2009) 11323–11325.
[33] K.J. Davies, J. Biol. Chem. 262 (1987) 9895–9901.
[34] W.M. Garrison, Chem. Rev. 87 (1987) 381–398.
[35] M. Gracanin, C.L. Hawkins, D.I. Pattison, M.J. Davies, Free Radic. Biol. Med. 47 (2009) 92–102.
[36] S. Fu, S. Gebicki, W. Jessup, J.M. Gebicki, R.T. Dean, Biochem. J. 311 (1995) 821–827.
[37] A. Wright, W.A. Bubb, C.L. Hawkins, M.J. Davies, Photochem. Photobiol. 76 (2002) 35–46.
[38] J.M. Marsh, M.G. Davis, M.J. Flagler, Y. Sun, T. Chaudhary, M. Mamak, D. W. McComb, R.E.A. Williams, K.D. Greis, L. Rubio, L. Coderch, Int. J. Cosmet. Sci. 37 (2015) 532–541.